

Au-Pd Alloy Nanoparticles Catalyze the Colorimetric Detection of Hydrazine with Methylene Blue

Wei Liu†, Guangchao Zheng†, Wing-Leung Wong and Kwok-Yin Wong*

State Key Laboratory of Chemical Biology and Drug Discovery, Department of Applied Biology and Chemical Technology, The Hong Kong Polytechnic University, Hung Hom, Kowloon, Hong Kong, China

* Corresponding author

E-mail: kwok-yin.wong@polyu.edu.hk

† These authors contributed equally to this study

Abstract

A colorimetric detection of hydrazine with methylene blue (methylthioninium chloride) as redox indicator using Au-Pd alloy nanoparticles (NPs) as catalyst is described. Contrary to Au or Pd NPs which are not active to induce a rapid color change, the Au-Pd alloy NPs allow for a fast response of the sensing system within a few minutes at room temperature. A linear change in absorbance versus hydrazine concentration ranging from 0.1 to 5.0 mM can be obtained. The catalytic activity of the Au-Pd alloy NPs in the reaction can be attributed to the electronic inductive effect by Au on Pd in the alloy NPs.

Introduction

Metal nanomaterials show to possess distinct and desirable properties compared with their bulk materials [1]. For example, the active surface in Pd nanomaterials has contributed to several catalyzed organic reactions [2-5] and electrochemical sensing systems [6-8]. Note that some metal alloy nanomaterials are superior in catalytic activity to their single metal counterparts, much work has been carried out to develop metal alloys. Among them, Au-Pd nanomaterials have received many interests in catalytic reaction and sensing, for example, plasmon-enhanced spectroscopic detection of hydrogen gas [9-11].

As an industrial agent, hydrazine has been widely used as a foam-blowing agent in polymerization process and as an agricultural pesticide. However, hydrazine has been classified as a Group 2A probable human carcinogen by International Agency for Research of Cancer (IARC) due to the high toxic nature [12, 13]. The improper discharge or leaking of hydrazine may cause serious public health issues, hereby making the detection of hydrazine urgent and driving an exploration on active catalyst for this purpose. To date, much work on Pd nanoparticles (NPs) has shown to be effective on hydrazine detection by electrochemical sensors [14-17]. Zare *et al.* firstly discovered the decreased oxidation overpotential of hydrazine in the presence of Pd NPs [14]. Yang *et al.* further introduced a sensitive and durable electrochemical sensing platform by anchoring Pd NPs on CoAl-layered double hydroxide for the detection of hydrazine [15]. Compton *et al.* reported that the Pd supported on carbonaceous materials are highly-active and stable electrocatalyst for hydrazine oxidation [16,17]. Moreover, Nunes *et al.* demonstrated that a high-oxidation state molybdenum-complex can be applied to the spectroscopic detection of hydrazine [18]. Despite well-documented applications of Pd NPs from literature, the colorimetric detection of hydrazine by metal NPs has not been reported.

In this communication, Au-Pd alloy NPs are studied for the colorimetric detection of hydrazine through its decomposition in the presence of a redox indicator methylene blue (methylthioninium chloride). In the system, the blue redox indicator is reduced to its colorless form (leucomethylthioninium) revealing the presence of hydrazine under room temperature condition. The effectiveness of the Au-Pd alloy NPs can be attributed to the electronic inductive effect by Au on Pd, [19] which may generate a highly-active surface for the catalytic reaction.

Experimental Section

Materials: Chemicals were purchased from Sigma-Aldrich and were used without further purification except vacuum drying. Milli-Q deionized (D.I.) water was used throughout the preparation and in all experiments.

Instrumentation: UV–Vis absorption spectra were recorded on a Hewlett Packard Model 8453 Diode Array UV-Vis Spectrophotometer. The sample solutions were prepared with D.I. water using a quartz cuvette of 1 cm path length. TEM images were obtained using a scanning TEM (JEOL JEM-2100F) operated with a field emission gun at 200 kV. The samples were drop-cast onto holey carbon-coated 400 mesh copper grids before TEM imaging. The elemental compositions of materials were characterized by an energy dispersive spectrometer (EDS) attached to the TEM.

Synthesis of metal and metal alloy NPs: The synthetic procedures of the Au-Pd alloy NPs followed the literature report [20] with slight modification. To Pd(OAc)₂ (10 mM, 1 mL) in HCl solution (37 %) in a flask cooled in an ice-bath, HAuCl₄ aqueous solution (10 mM, 1.5 mL) was added and the mixture was stirred for 10 min. Then, L-ascorbic acid (50 mM, 2 mL) was added to the above solution with vigorous stirring for 10 min. Subsequently, aqueous NaBH₄ solution (10 mM, 0.5 mL) was added dropwise over a period of 10 min. The color of solution turned gradually from brown to dark grey, indicating the formation of colloidal Au-Pd NPs in the aqueous solution. Pd and Au NPs were synthesized using similar procedures but with only one metal source.

Colorimetric detection of hydrazine: To a 10 mL flask was transferred a certain volume of solution containing Au-Pd alloy NPs, 1 ml of 8 M hydrochloric acid, 0.5 ml of 0.16 mM methylthioninium chloride and the volume as adjusted to 3 ml with D.I. water. Then, 1 ml of 3 M hydrazine monochloride solution was added. The absorption spectra of the mixture against time were measured immediately after the addition of hydrazine monochloride solution.

Results and discussion

Catalyst with high activity is essential in the construction of rapid-sensing system for the detection of target analytes because the catalyst can efficiently amplify the signal changes through a catalytic reaction to transform signaling molecules from one form to another. Methylene blue or methylthioninium chloride is used as a redox indicator, which can be turned to colorless when reduced to leucomethylthioninium. This color change from blue to colorless is visually observable. However, the redox process on methylene blue cannot proceed rapidly with hydrazine as it is a weak reducing agent. A suitable catalyst should be introduced to the redox reaction, and thus a sensing system for colorimetric detection of hydrazine can be feasibly established. The system is sensitive with the color change of methylene blue observable even by naked eye. The working principle is shown in Figure 1.

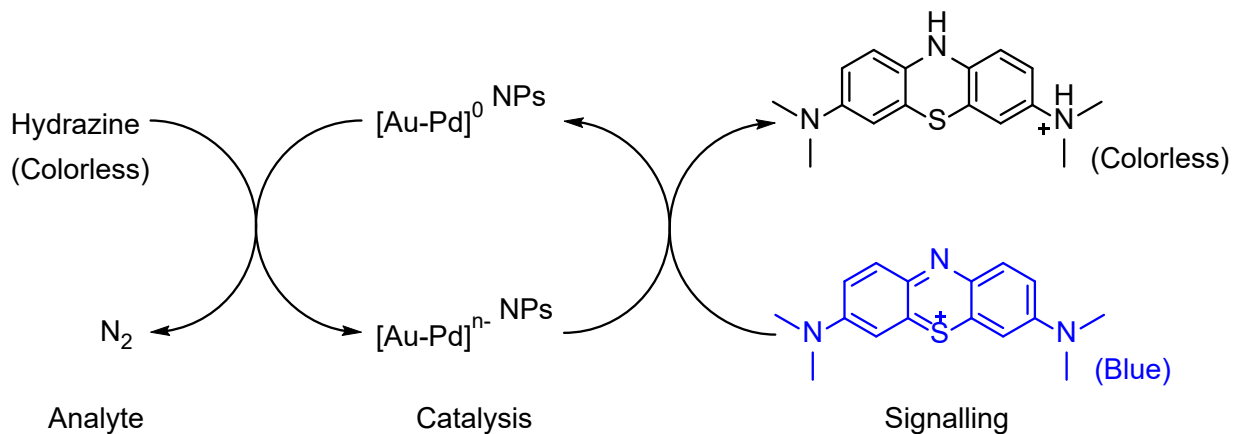


Figure 1. A sensing system based on Au-Pd NPs for the colorimetric detection of hydrazine.

Au-Pd, Au, and Pd NPs were synthesized and compared for their catalytic performance in the colorimetric detection of hydrazine. The nanostructures of obtained NPs are firstly studied by transmission electron microscopy (TEM) images, which are shown in Figure 2. Different morphologies and particle sizes can be clearly seen from the images, though they were prepared by similar conditions with L-ascorbic acid as the capping ligand and $NaBH_4$ as the reducing agent. The Au NPs are of oval-like polyhedron shape with a size dominantly of 54.7 nm (Figure 2: a, b) while the Pd NPs are more spherical in shape with a rough surface and their majority size is 37.9 nm approximately (Figure 2: c, d). Interestingly, the alloy of Au-Pd gave completely different particle shape and size, which were found to be nanoparticle clusters with smooth

surfaces (Figure 2: e, f) and the particle size ranged from 40-110 nm (majority size 98.4 nm) which is much bigger than the Au NPs and Pd NPs (Figure S1). The lattice planes of these NPs can be observed from the close-up images in Figure 2: b, d, f. The d -spacing for adjacent lattice planes measured from 3 different places on a single Au-Pd NP was 0.23 nm, which corresponds to the mean value of the (111) planes of face-centered cubic (fcc) Au and Pd. This value also agrees with that of the (111) planes of fcc bulk Au-Pd alloy from the literature [21]. The atomic ratio of Au:Pd of the Au-Pd NPs as measured by energy dispersive spectrometer (EDS) is 57:43 (Figure S2).

To further characterize the Au-Pd alloy NPs, the elemental distribution of a selected Au-Pd NP was carried out by scanning transmission electron microscopy (STEM). The elemental distribution mapping of Au, Pd, and merged Au-Pd on the selected nanoparticles were shown in Figure 3. The results show that both Au and Pd elements can be found from the selected nanoparticle as shown in the mapping image. From the merged image, both Au and Pd elements were detected across the body of the nanoparticle with uniform distribution, which confirms the resultant nanoparticles to be an alloy. Furthermore, the measured lattice spacings (0.23 nm) of Au-Pd NPs correspond to the mean value of the (111) planes of Au and Pd also in agreement with the Pd-rich case having the lattice spacing of 0.229 nm.[22] Since both Au and Pd are of *fcc* structure, the alloyed nanoparticle remains the *fcc* structure and therefore no discrepancy in lattice spacing is observed from the individual nanoparticle.

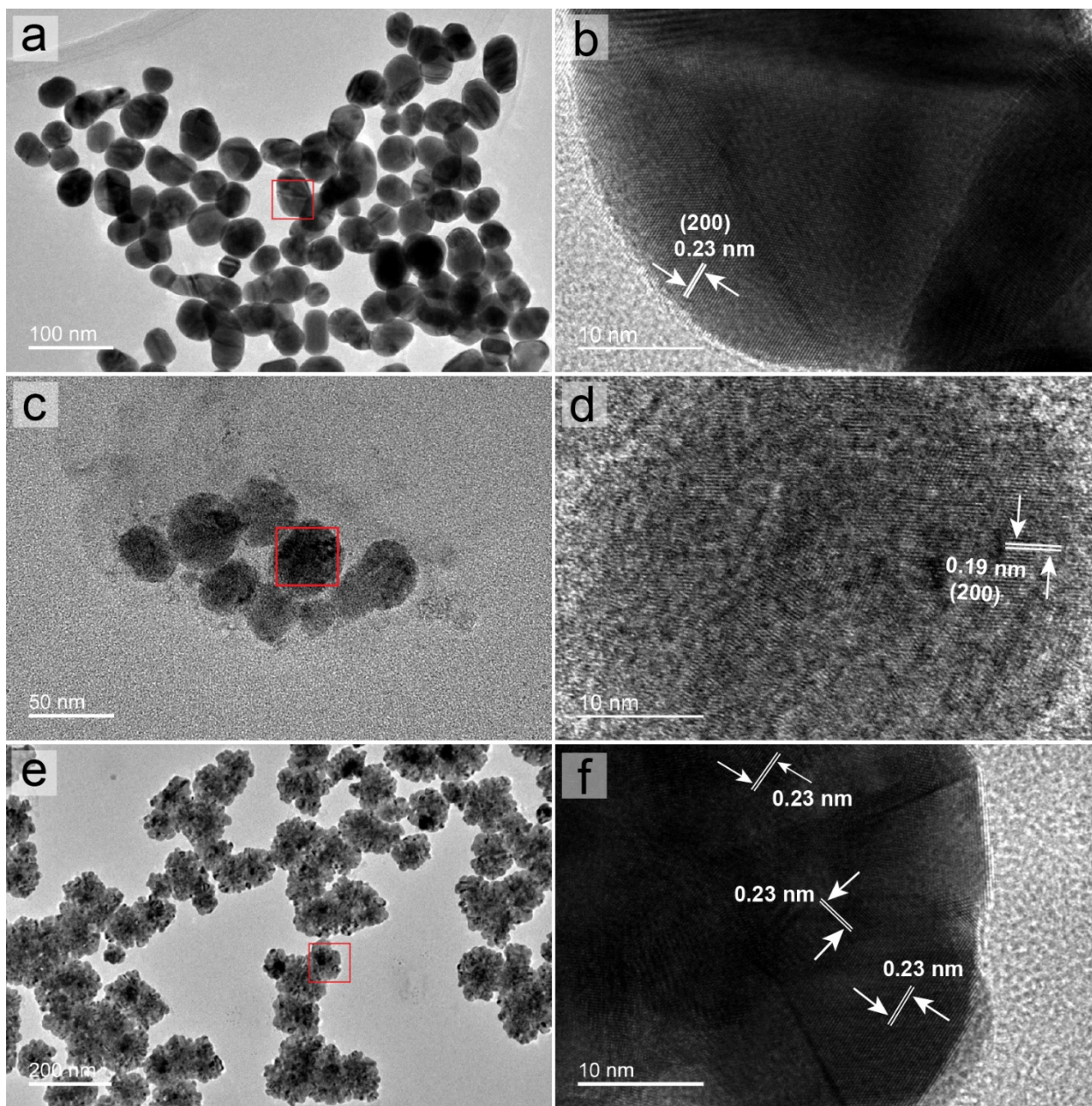


Figure 2. TEM images of (a) Au NP, (c) Pd NPs and (e) Au-Pd alloy NPs. (b), (d) and (f) are the close-up view of (a), (c) and (e) respectively.

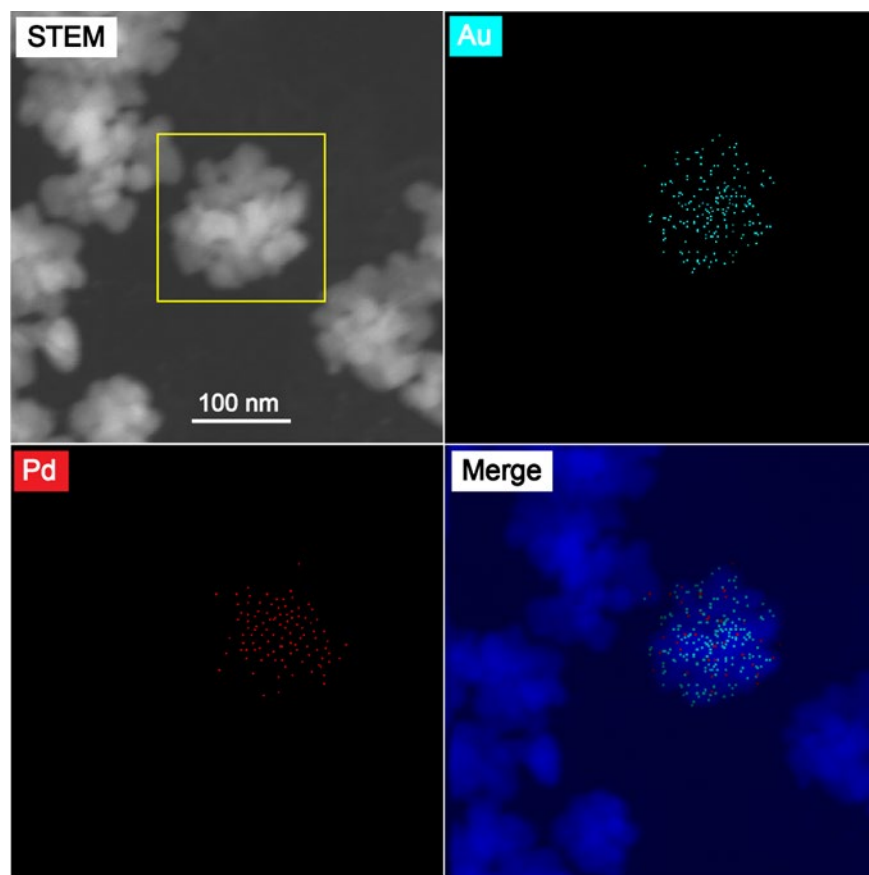


Figure 3. STEM image of a selected Au-Pd NP with elemental distribution of Au, Pd, and merged Au-Pd on the selected particle.

The optical properties of the above nanomaterials were investigated by UV–Vis absorption spectroscopy, and shown in Figure 4. Au NPs show a characteristic surface plasmon absorption at 520 nm, while Pd NPs typically shows no strong absorption peak in the UV–vis region (300–800 nm) which is in accordance with literature [23]. It is noteworthy that the Au-Pd NPs shows a suppressed plasmon band (ca. 550 nm), indicating that the introduction of Pd into Au caused a plasmon damping [24].

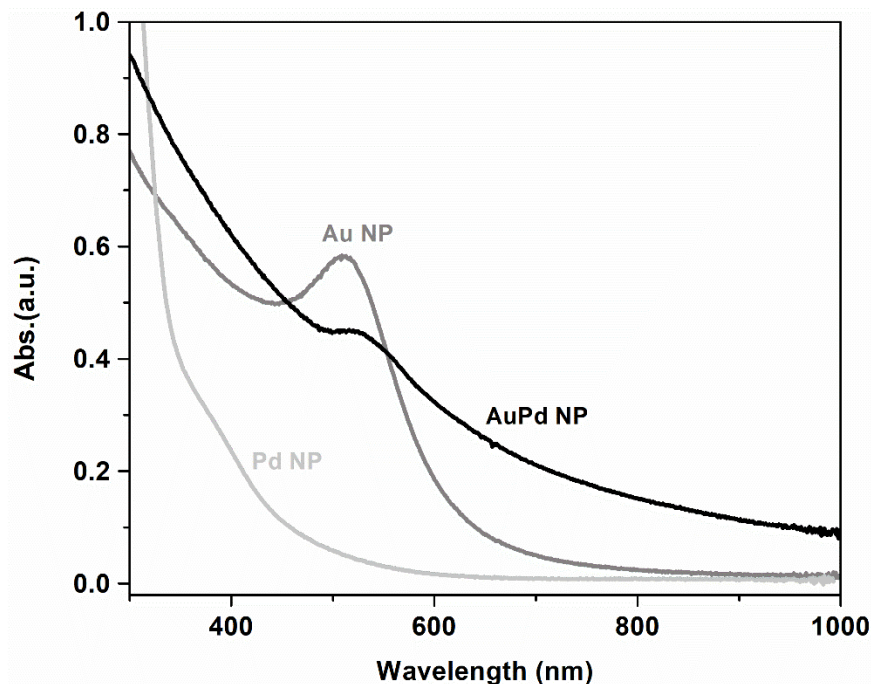


Figure 4. UV-vis-NIR absorption spectra of Au, Pd, and Au-Pd nanoparticles.

The catalytic activities of nanoparticles were investigated on the reaction of hydrazine decomposition and methylthioninium chloride reduction under acidic conditions. In this catalytic reaction system, the reduction of methylthioninium chloride by the Au-Pd NPs catalyst showed remarkable color changes from blue to colorless, which can be represented by the UV-Vis absorption changes observed in the visible range of 600 – 800 nm. Typical UV-Vis absorption changes of methylthioninium chloride (20 μ M) with Au-Pd NPs as the catalyst (10 μ g) in the presence of hydrazine (0.75 M) with reaction time are shown in Figure 5. The absorption maxima (λ_{max}) at 750 nm were found to decrease gradually over time. Control experiments showed that no change in absorbance was observed in the absence of catalyst or hydrazine in the reaction system. In addition, the Au NPs showed no catalytic activity to cause a color change of the signal molecule (Figure S3); whereas the Pd NPs could only induce a much slower rate of decoloration (Figure S4) under the same experimental conditions. These results indicate that the obtained Au NPs and Pd NPs are much less reactive compared with Au-Pd NPs. This can probably be attributed to the geometric effect on Au-Pd and the electronic inductive effect of Au on Pd in the alloy NPs [19, 25]. A highly reductive species ($[\text{Au-Pd}]^{n-}$) as the electron-carrier is able to reduce the signal molecule rapidly to generate the color change of the test solution.

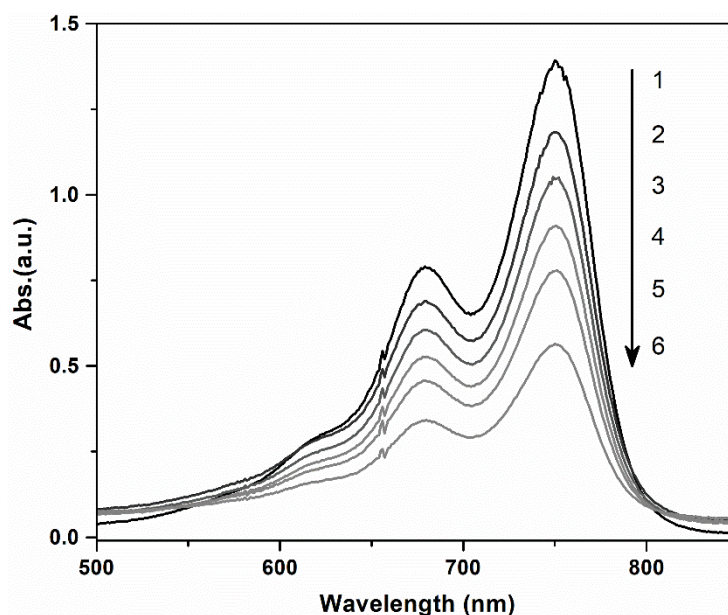


Figure 5. Absorbance changes of methylthioninium chloride for its reaction with hydrazine in the presence of Au-Pd NPs catalyst. Experimental conditions: Au-Pd NPs catalyst 10 μg ; methylthioninium chloride 20 μM ; hydrazine 0.75 M; hydrochloride acid 2 M. The experiments were conducted at room temperature. Time intervals set at 20 s for each measurement: (1) 0 s, (2) 20 s, (3) 40 s, (4) 60 s, (5) 80 s and (6) 100 s.

Concentrations of hydrazine in aqueous solution ranged from 0.05 M to 0.75 M were examined by this Au-Pd NPs sensing system. By monitoring the optical signal with λ_{max} at 750 nm, it was found that the higher the concentration of hydrazine, the faster was the de-coloration of the signal molecule (Figure S5). The catalytic reduction of methylthioninium chloride to leucomethylthioninium was found to be correlated with the concentration of hydrazine. For a low hydrazine concentration range of 0.1 mM to 5.0 mM (Figure 6), increasing the Au-Pd catalyst loading to 1 mg approximately could speed up the reaction. In addition, a good linear relationship of absorbance change $((A_0-A)/A_0)$ versus the concentrations of hydrazine can be established ($R^2 = 0.95$) as shown in Figure 6b. The limit of detection (LOD) estimated was 0.39 mM ($S/N = 3$), which is better than some of the reported Pd-based nano-materials for hydrazine detection (Table S1). Moreover, the rate of reaction follows an exponential equation: $y = Ae^{-kt} + y_0$, in which the factor k denotes a first-order reaction rate constant. The calculated rate constants are plotted against the concentrations of hydrazine and shown in Figure 6c.

The morphology of the Au-Pd NPs after the catalytic reaction was also examined with TEM and STEM (Figure S6). The images show no observable change in both morphology and shape of the Au-Pd NPs, indicating the robustness of nano-catalyst. Some common and moisture stable reducing agents, such as oxalic acid, formic acid and ascorbic acid, were also tested to investigate the potential interferences to the present sensing system. Only hydrazine can cause remarkable signal change in the catalytic reduction of methylthioninium chloride to leucomethylthioninium, while oxalic acid, formic acid and ascorbic acid give very weak reduction reaction under the same conditions (Figure S7). In addition, the performance of the sensing system was conducted with tap water and seawater (sample collected from Victoria Harbour, Hong Kong) as the reaction medium (Figure S8). In both cases, they showed comparable results with the case carried out in D.I. water. The result may suggest that the Au-Pd NPs sensing system is not sensitive to the salts, impurities and pollutants present in the practical environment.

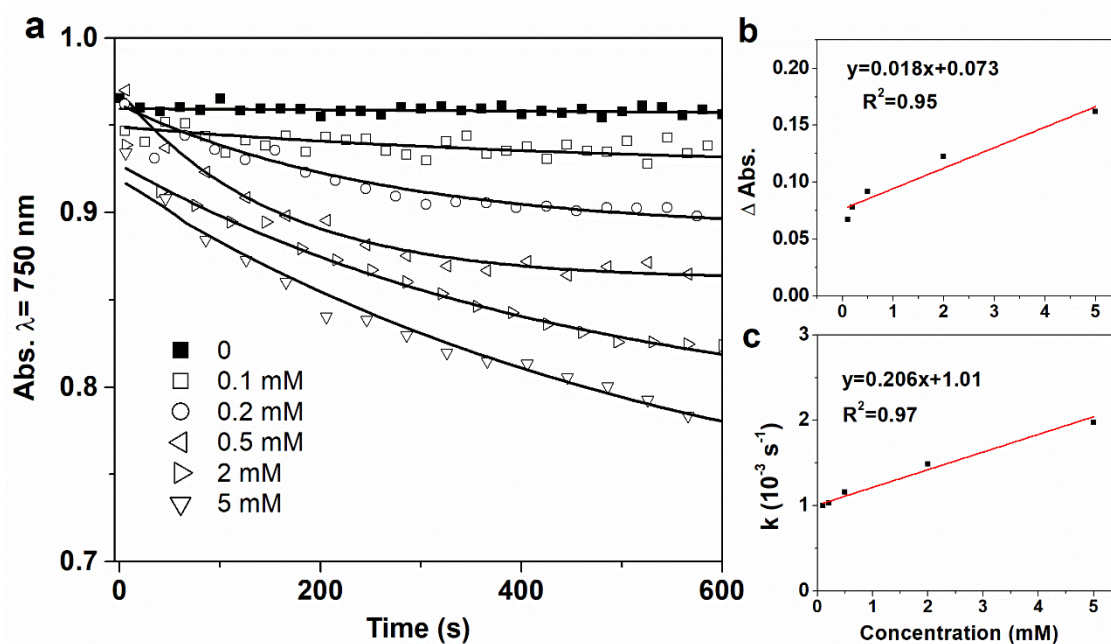


Figure 6. (a) Effect of hydrazine concentrations on the absorbance change at 750 nm in the catalytic reaction; (b) a linear relationship of absorbance changes at $t=480$ s against the concentration of hydrazine; and (c) a linear relationship of calculated first-order rate constants against the concentration of hydrazine. Experimental conditions: Au-Pd catalyst 1 mg;

methylthionium chloride 16 μ M; hydrochloride acid 2 M. The experiments were conducted at room temperature.

Conclusion

In conclusion, a new colorimetric sensing system based on Au-Pd alloy nanoparticles for rapid detection of hydrazine in aqueous medium was established using methylthionium chloride as the indicator. Hydrazine in the concentration range of 0.1 mM to 5.0 mM could be detected with a linear response of signal changes. In addition, this study demonstrated a significant catalytic enhancement from Au-Pd alloy nanoparticles that facilitate a rapid sensing of hydrazine at low concentration in aqueous medium, which cannot be achieved with Au or Pd NPs alone under similar conditions.

Acknowledgment

We acknowledge the support from the Innovation and Technology Commission of Hong Kong and The Hong Kong Polytechnic University. KYW acknowledges the support from the Patrick S.C. Poon endowed professorship.

References

1. The Chemistry of Nanomaterials: Synthesis, Properties and Applications. C. N. R. Rao, A. Müller and A. K. Cheetham ed., Wiley-VCH (2005).
2. A. J. Reay, I. J. S. Fairlamb, Catalytic C-H bond functionalisation chemistry: the case for quasi-heterogeneous catalysis, *Chem. Commun.* 51 (2015) 16289-16307.
3. A. M. Trzeciak, A. W. Augustyniak, The role of palladium nanoparticles in catalytic C-C cross-coupling reactions, *Coord. Chem. Rev.* 384 (2019) 1-20.
4. G. Zheng, K. Kaefer, S. Mourdikoudis, L. Polavarapu, B. Vaz, S.E. Cartmell, A. Bouleghimat, N.J. Buurma, L. Yate, A.R. de Lera, L.M. Liz-Marzán, I. Pastoriza-Santos and J. Pérez-Juste. Palladium nanoparticle-loaded cellulose paper: A highly efficient, robust, and recyclable self-assembled composite catalytic system. *J. Phys. Chem. Lett.* 6 (2014) 230-238.
5. M. Bagherzadeh, F. Ashouri, L. Hashemi, A. Morsali, Supported Pd nanoparticles on Mn-based metal-organic coordination polymer: Efficient and recyclable heterogeneous catalyst for Mizoroki-Heck cross coupling reaction of terminal alkenes, *Inorg. Chem. Commun.* 44 (2014) 10-14.
6. S. K. Kim, S. Jeon, Simultaneous determination of serotonin and dopamine at the PEDOP/MWCNTs-Pd nanoparticle modified glassy carbon electrode, *J. Nanosci. Nanotechnol.* 12 (2012) 1903-1909.

7. A. Shaikh, S. Parida, Facile sonochemical synthesis of highly dispersed ultrafine Pd nanoparticle decorated carbon nano-onions with high metal loading and enhanced electrocatalytic activity, *RSC Adv* 6 (2016) 83711-83719.
8. J. Wang, H. Sun, H. Pan, Y. Ding, J. Wan, G. Wang, M. Han, Detection of hydrogen peroxide at a palladium nanoparticle-bilayer graphene hybrid-modified electrode, *Sens. Actuat. B Chem.* 230 (2016) 690-696.
9. N. Liu, M.L. Tang, M. Hentschel, H. Giessen and A. P. Alivisatos. Nanoantenna-enhanced gas sensing in a single tailored nanofocus. *Nature Materials*, 10 (2011) 631-636.
10. A. Tittl, P. Mai, R. Taubert, D. Dregely, N. Liu and H. Giessen, Palladium-based plasmonic perfect absorber in the visible wavelength range and its application to hydrogen sensing, *Nano Lett.*, 11 (2011) 4366–4369.
11. S. Rodal-Cedeira, V. Montes-García, L. Polavarapu, D.M. Solís, H. Heidari, A. La Porta, M. Angiola, A. Martucci, J.M. Taboada, F. Obelleiro, S. Bals, J. Pérez-Juste and I. Pastoriza-Santos. Plasmonic Au@Pd nanorods with boosted refractive index susceptibility and SERS efficiency: A multifunctional platform for hydrogen sensing and monitoring of catalytic reactions, *Chem. Mater.* 28 (2016) 9169-9180.
12. IARC monographs on the identification of carcinogenic hazards to humans, vol. 4, Sup. 7, 11, 115 (2018).
13. OSHA Occupational Chemical Database, The Occupational Safety and Health Administration, USA (2018), <https://www.osha.gov/chemicaldata/>
14. N. Daryanavard, H. R. Zare, Single palladium nanoparticle collisions detection through chronopotentiometric method: introducing a new approach to improve the analytical signals, *Anal. Chem.* 89 (2017) 8901-8907.
15. L. Xu, Z. Qu, J. Chen, X. Chen, F. Li, W. Yang, Highly dispersed palladium nanoparticles generated in situ on layered double hydroxide nanowalls for ultrasensitive electrochemical detection of hydrazine, *Anal. Methods* 9 (2017) 6629-6635.
16. J. Panchompoo, L. Aldous, C. Downing, A. Crossley, R. G. Compton, Facile synthesis of Pd nanoparticle modified carbon black for electroanalysis: Application to the detection of hydrazine, *Electroanal.* 23 (2011) 1568-1578.
17. X. Ji, C. E. Banks, A. F. Holloway, K. Jurkschat, C. A. Thorogood, G. C. Wildgoose, R. G. Compton, Palladium sub-nanoparticle decorated 'bamboo' multi-walled carbon nanotubes exhibit electrochemical metastability: voltammetric sensing in otherwise inaccessible pH ranges, *Electroanal.* 18 (2006) 2481-2485.
18. H. Vrabel, V. H. C. Verzenhassi, S. Nakagaki, F. S. Nunes, Catalytic reduction of hydrazine to ammonia by a high-oxidation state molybdenum complex, *Inorg. Chem. Commun.* 11 (2008) 1040–1043.
19. V. Pallassana, M. Neurock. Electronic factors governing ethylene hydrogenation and dehydrogenation activity of pseudomorphic Pd_{ML}/Re(0001), Pd_{ML}/Ru(0001), Pd(111), and Pd_{ML}/Au(111) surfaces, *J. Catal.* 191 (2000) 301-317.

20. J. Chai, F. Li, Y. Hu, Q. Zhang, D. Han, L. Niu, Hollow flower-like Au-Pd alloy nanoparticles: One step synthesis, self-assembly on ionic liquid-functionalized graphene, and electrooxidation of formic acid, *J. Mater. Chem.* 21 (2011) 17922-17929.
21. S.C. Tsen, P.A. Crozier, J. Liu, Lattice measurement and alloy compositions in metal and bimetallic nanoparticles, *Ultramicroscopy* 98 (2003) 63-72.
22. D. Wang, A. Villa, F. Porta, L. Prati, D. S. Su, Bimetallic gold/palladium catalysts: correlation between nanostructure and synergistic effects, *J. Phys. Chem. C* 112 (2008) 8617-8622.
23. M. Önder, X. Sun, S. Sun, Monodisperse gold-palladium alloy nanoparticles and their composition-controlled catalysis in formic acid dehydrogenation under mild conditions, *Nanoscale* 5 (2013) 910-912.
24. H. Chen, F. Wang, K. Li, K.C. Woo, J. Wang, Q. Li, L. D. Sun, X. Zhang, H. Q. Lin, C. H. Yan, Plasmonic percolation: plasmon-manifested dielectric-to-metal transition, *ACS Nano*, 8 (2012) 7162-7171.
25. M. O. Nutt, J.B. Hughes, M. S. Wong, Designing Pd-on-Au bimetallic nanoparticle catalysts for trichloroethene hydrodechlorination, *Environ. Sci. Technol.* 39 (2005) 1346-1353.

Supporting Information

Au-Pd Alloy Nanoparticles Catalyzes the Colorimetric Detection of Hydrazine with Methylene Blue

Wei Liu[†], Guangchao Zheng[†], Wing-Leung Wong and Kwok-Yin Wong*

State Key Laboratory of Chemical Biology and Drug Discovery, Department of Applied Biology and Chemical Technology, The Hong Kong Polytechnic University, Hung Hom, Kowloon, Hong Kong, P.R. China

* Corresponding author

E-mail: kwok-yin.wong@polyu.edu.hk

[†] The authors contributed equally to this study

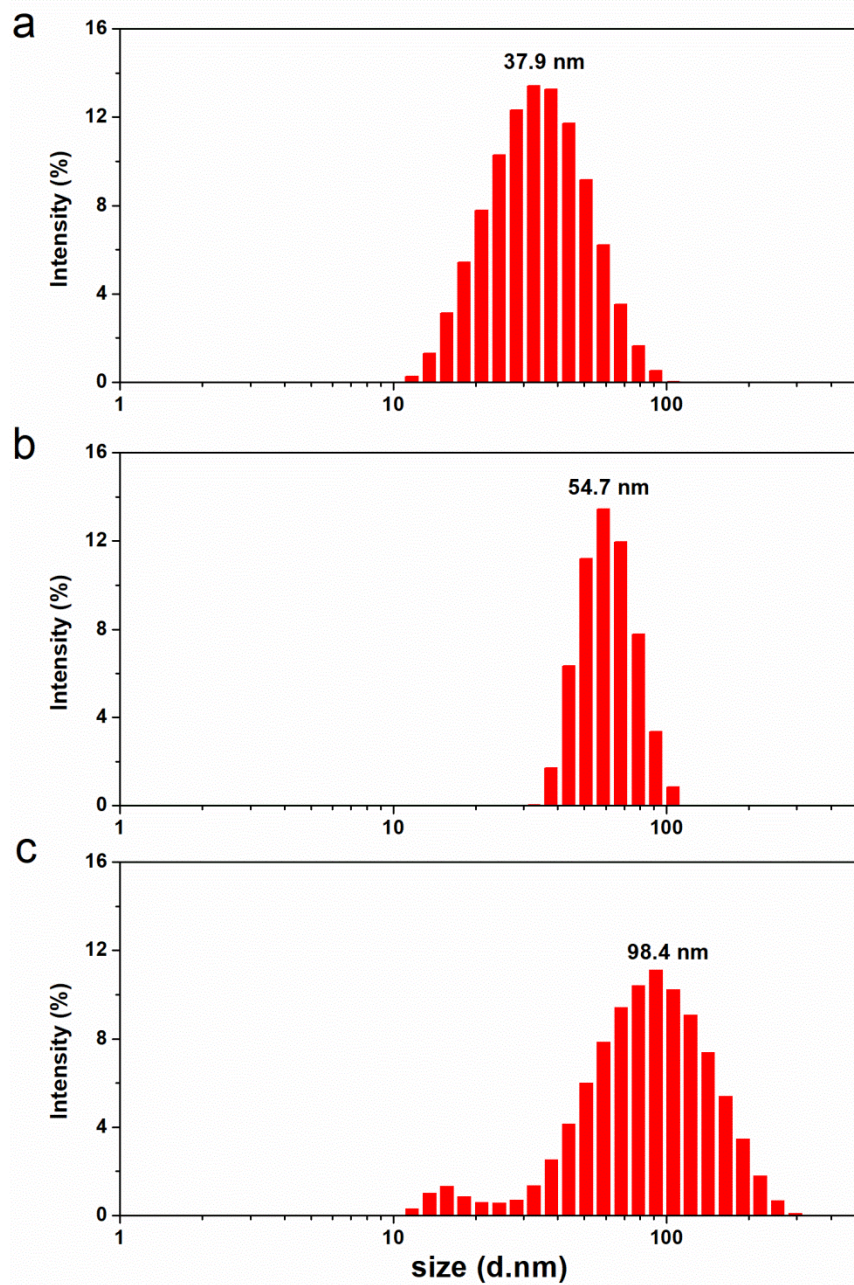


Figure S1. The size distribution of the synthesized nanoparticles: (a) Pd NPs, (b) Au NPs, and (c) Au-Pd NPs.

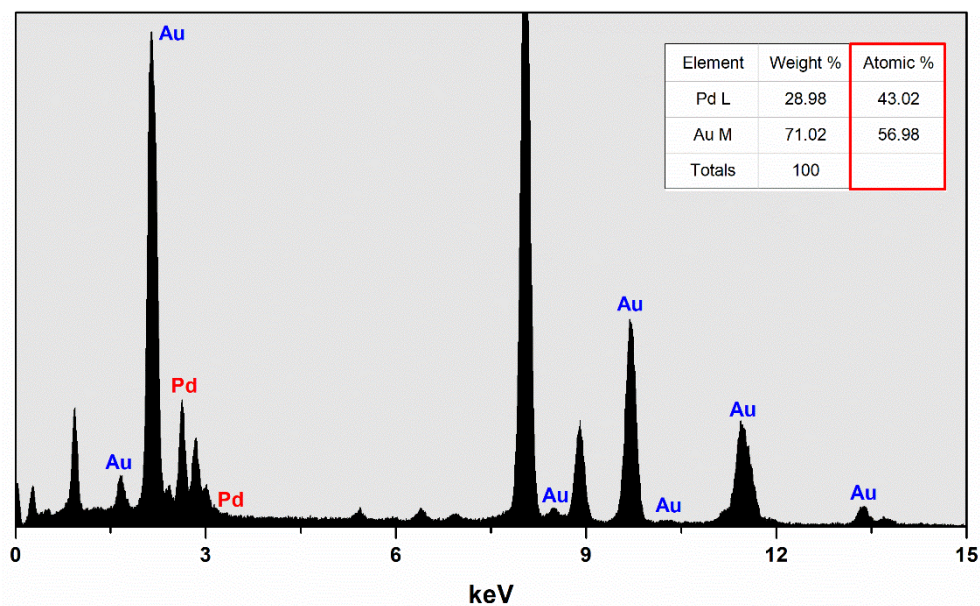


Figure S2. EDS diagram showing the elemental content in the Au-Pd NPs.

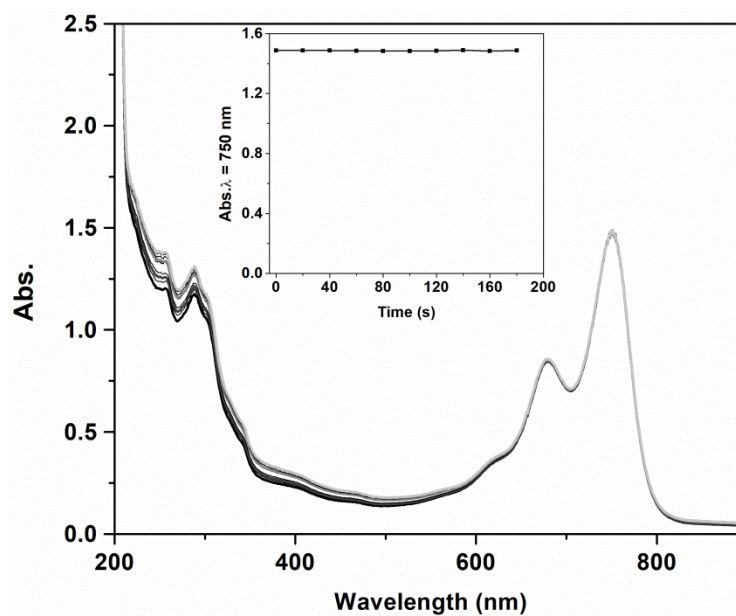


Figure S3. Absorbance changes of methylthioninium chloride versus time for the reaction with hydrazine in the presence of Au NPs catalyst. Experimental conditions: Au catalyst 10 μg ; methylthioninium chloride 20 μM ; hydrazine 0.75 M; hydrochloride acid 2 M. The experiments were conducted at room temperature. Time intervals set at 20 s for each measurement.

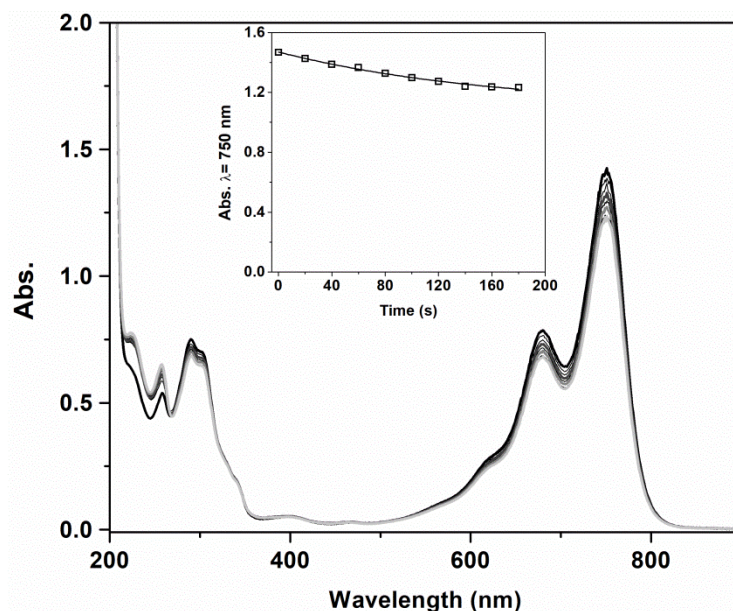


Figure S4. Absorbance changes of methylthioninium chloride versus time for the reaction with hydrazine in the presence of Pd NPs catalyst. Experimental conditions: Pd catalyst 10 μg ; methylthioninium chloride 20 μM ; hydrazine 0.75 M; hydrochloride acid 2 M. The experiments were conducted at room temperature. Time intervals set at 20 s for each measurement.

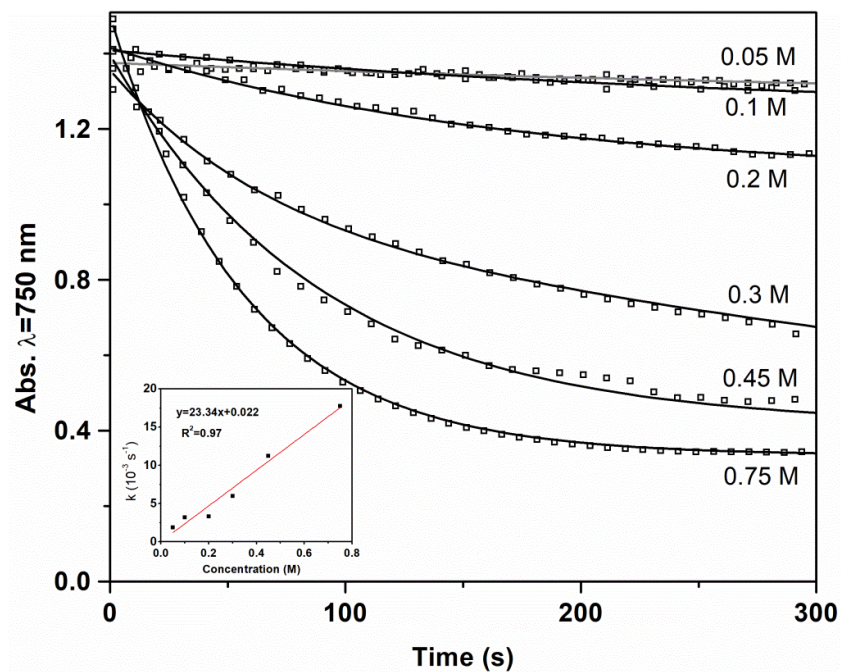


Figure S5. Effect of hydrazine concentrations on the absorbance changes at 750 nm in the catalytic reaction. Conditions: Catalyst 10 μg ; methylthioninium chloride 20 μM ; hydrochloride acid 2 M; room temperature.

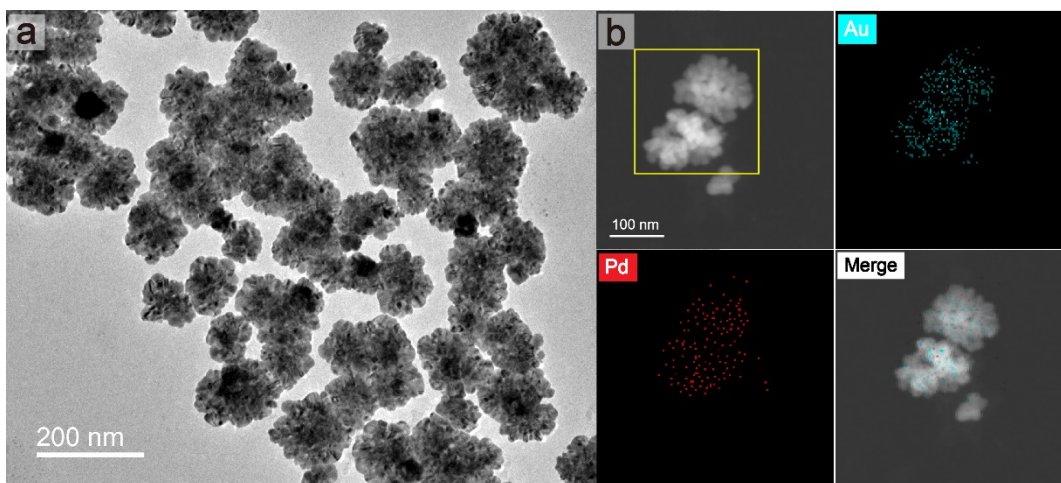


Figure S6. a) TEM image and b) STEM image of Au-Pd NPs with elemental mappings of Au, Pd, and two elements in merge after catalytic reactions.

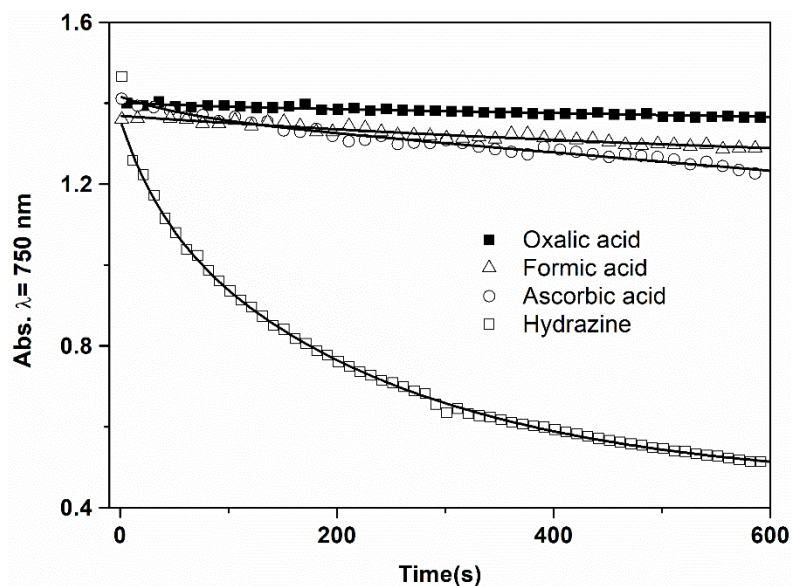


Figure S7. The study of some potential interference possibly from common reducing agents: oxalic acid, formic acid and ascorbic acid.

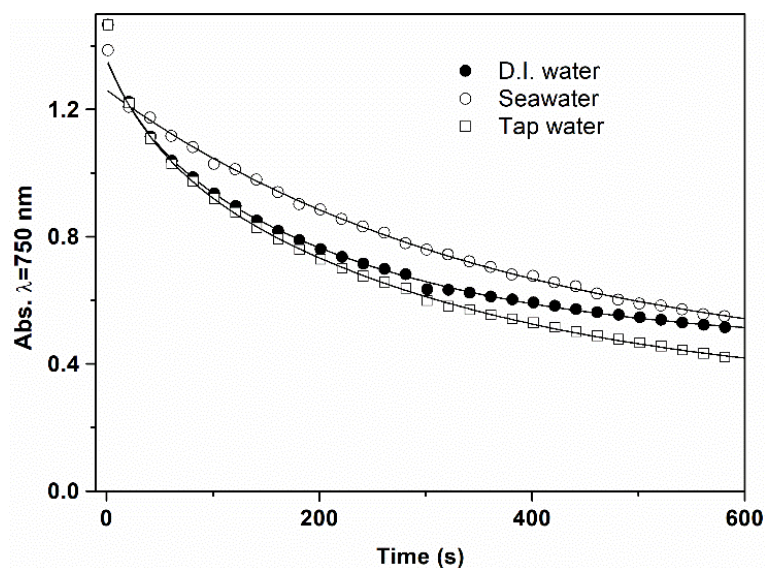


Figure S8. The comparison of the performance of the Au-Pd alloy catalyzed sensing system applied in de-ionized water, tap water and seawater.

Table S1. The comparison of LOD for the Pd based nano-materials for the detection of hydrazine.

Pd-based nano-materials	LOD	Reference
Pd/LSGCNs: Electrochemical sensor based on palladium loaded laser scribed graphitic carbon nanosheets	0.01 mM (0.32 ppm)	[1]
PdNP/LDHNW/ITO: CoAl-layered double hydroxide nanowall-supported Pd nanoparticle	0.01 μ M (0.00032 ppm)	[2]
Pd/CB: Pd Nanoparticle Modified Carbon Black	8.8 mM (281.6 ppm)	[3]
Pd/ MWCNTs: Palladium decorated bamboo MWCNTs	10 mM (320 ppm)	[4]
Au-Pd NPs: Au-Pd Alloy Nanoparticles Catalyst	0.39 mM (12.5 ppm)	This work

Reference:

- [1]. Y. Zhang, J. Ye. Electrochemical sensor based on palladium loaded laser scribed graphitic carbon nanosheets for ultrasensitive detection of hydrazine. *New J. Chem.*, 2018, 42, 13744-13753.
- [2]. L. Xu, Z. Qu, J. Chen, X. Chen, F. Li, W. Yang. Highly dispersed palladium nanoparticles generated in situ on layered double hydroxide nanowalls for ultrasensitive electrochemical detection of hydrazine. *Anal. Methods*, 2017, 9, 6629-6635.
- [3]. J. Panchompoo, L. Aldous, C. Downing, A. Crossley, R. G. Compton. Facile Synthesis of Pd Nanoparticle Modified Carbon Black for Electroanalysis: Application to the Detection of Hydrazine. *Electroanal.*, 2011, 23, 1568-1578.
- [4]. X. Ji, C. E. Banks, A. F. Holloway, K. Jurkschat, C. A. Thorogood, G. C. Wildgoose, R. G. Compton, Palladium sub-nanoparticle decorated 'bamboo' multi-walled carbon nanotubes exhibit electrochemical metastability: voltammetric sensing in otherwise inaccessible pH ranges, *Electroanal.*, 2006, 18, 2481-2485.